PROTON EMITTER STUDIES IN THE REGION OF Z > 50

V.A. Karnaukhov, D.D. Bogdanov and L.A. Petrov,
Joint Institute for Nuclear Research,
Dubna, USSR.

The present report consists of two parts. In the first part possibilities of obtaining nuclear information by means of delayed proton emitters are considered, in the second one our first results on the search for the proton decay from the nuclear ground state are presented. The advantages of nuclei in the region of $Z > 50$, compared to lighter ones, are not of principle, however, as will be seen below, they really exist and make heavy nuclei, in some respect, more predominant.

I. DELAYED PROTON EMITTERS

I.I. Introduction

Since the time of the first detection of the delayed proton emission[I] more than two dozens of proton emitters were discovered. The heaviest of them were recently produced. Delayed proton emitters among the isotopes of rare - earth elements have been synthesized in nuclear reactions induced by accelerated S^{32} and Cl^{35} ions (see the second part of the report). The heaviest isotopes decaying with proton emission (Hg ^{I8I}, ^{I83})have recently been detected as a product of spallation of lead by a team at the ISOLDE[2]

There is no doubt that delayed proton emitters may be found

for the majority of elements, except for possibly the re - gion of $Z > 83$ where the β^+ decay is suppressed with the alpha decay.

Fig. I gives an illustrative scheme of a decay re - sulting in delayed proton emission. The beta decay of a nucleus with large neutron deficiency leads to proton unstable levels being populated in the energy interval of a few MeV. The shape of the proton spectrum for relatively heavy nuc - lei is shown in Fig.I. The averaged spectrum exhibits a gross peak. If the resolution is high enough the spectrum reveals a fine structure which is due to the levels of the daughter nucleus [3,4].

I.2. Gross Treatment of Proton Spectra

The gross structure of the proton spectrum is direc- ly related to the one of the beta decay. This question has been analysed in detail in refs.[3,5]. The shape of the averaged spectrum of delayed protons can be presented as fol - lows:

$$\frac{\Delta N_p}{\Delta E_p} = \sum_{i,\gamma} F_{\beta^+,K}\,(Q_0 - B_p - E_p)\,\frac{\langle M^2\rangle}{D(E_p+B_p,\gamma)}\left\langle \frac{\Gamma_{p\gamma}^{(i)}}{\Gamma_\gamma}\right\rangle$$

where $F_{\beta^+,K}$ is the usual statistical rate function, Q_0 the total K-capture energy, $\langle M^2\rangle$ the squared matrix element averaged over the levels in the energy interval $\Delta E = \Delta E_p$, D the mean level spacing, Γ_p/Γ the relative proton width. The latter is essential only for the low-energy part of the spectrum and can be calculated by statistical model formulas. Thus, the averaged spectrum analysis may yield some information on the beta transition strength function.

The theoretical importance of the investigation of the averaged beta-decay properties has been shown by a number of authors (e.g. refs.[6,7]) and is discussed in detail in the report by Yamada at this Conference.

In Figs. 2 and 3 examples of averaged proton spectra (Te^{III} and Te^{I09}) are given. The continuous curves are calculated under the assumption that the strength function is constant. The result fits well with experiment. Thus, in the case of Te^{III} the deviation of the experimental points from the calculated curve does not exceed 40 % for a complete change of the intensity in the spectrum by a factor of I00. The constancy of the strength function does not contradict theoretical predictions. According to the theoretical consideration[6,7], the Gamow-Teller strength function has giant resonance shape. The peak energy of it is located near the isobaric analogue state. The excitation energy region of interest (3-7 MeV) contains only the tail of this resonance. Therefore the constant value of the strength function is a good approximation.

Fig . 2a gives also the result of the calculation performed under the assumption $\langle M^2 \rangle$ = const. (exponential increase of the strength function with energy) that was extensively used to date in delayed neutron calculations. The inconsistency of this assumption is quite obvious.

I.3. Delayed Protons and Mass Formulas

It seems useful to employ delayed proton spectra for checking mass formula calculations in the region of nuc -

lei with large neutron deficiency. At present several me - thods are known for the calculation of nuclear masses. For isotopes near the stability line, the difference between these approaches is insignificant and does not solve the problem which of them should be preferred. However, in extrapolating calculations to a far off stability region, the results essentially diverge and the experimental check in this region may be crucial.

The shape of the average proton spectrum depends upon the two energy parameters : proton binding energy, B_p, of the intermediate nucleus and total $\beta^+ - p$ decay energy $Q_0 - B_p$ The latter coincides also with the binding energy difference of the initial and final nuclei. The B_p value defines the low-energy part of the spectrum and the position of the gross-maximum. The shape of the spectrum to the right from the gross maximum depends mainly upon the $Q_0 - B_p$ value. Both parameters can be determined by comparing the calculated and experimental proton spectra.

The quantity $Q_0 - B_p$ can be measured in a separate experiment, as well. In ref.[8] it has been found for Te^{III} with a good accuracy by comparing the proton spectra in coincidences with positons and without coincidences. The intensity ratio is unambiguous determined by the β^+/K branching ratio which depends upon the partial transition energy $Q = Q_0 - B_p - E_p$. Thus, for Te^{III} $Q_0 - B_p$ was found to be 5.07 ± 0.07 MeV. The accuracy of the determination of $Q_0 - B_p$ from the gross spectrum is somewhat worse.

Table I shows the experimental and calculated decay energies for Te^{III} and Te^{I09}.

Table I

	Exp.MeV	C.	S.	S.-M.	W.-V.	Z.	G.-K.	N.
Q_o-B_p ($Te^{III}-Sb^{III}$)	5.07±0.07	6.7	6.0	6.I5	2.5	4.9	5.07	5.5
$B_p(Sb^{III})$	I.83±0.20	I.6	I.6	I.75	3.2	2.I	I.78	2.I
Q_o-B_p ($Te^{I09}-Sb^{I09}$)	7.6±0.4	8.9	8.2	8.4	4.0	6.95	6.94	7.8
$B_p(Sb^{I09})$	I.0±0.3	0.7	0.8	0.9	2.8	I.3	I.I4	I.3

C. - Cameron, A.G.W.[9]

S. - Seeger, P.[I0]

S.-M. - Swiatecki, W., Myers, W.[II]

Z. - Zeldes, N. et al.[I3]

G.-K.-Garvey,G., Kelson,I.[I4] et al.

W.-V.-Wing,J., Varley, J.[I2]

N.-Nemirovski[I5]

Thus, in the region around the double closed shell of Z=N=50 the calculations performed by Zeldes et al[I3], Garvey et al[I4], Nemirovski[I5] seem to work the best.

I.4. Fine Structure of the Proton Spectrum

Now let us consider the deviations of the experimental spectra from the calculated ones. First of all, we should indicate the intermediate structure which is displayed in spectra with poor resolution (ΔE_p= 300 KeV) This structure appears to be due to simple states of the daughter nucleus favouring the beta decay. Thus, for example in the Te^{109} spectrum there is observed a relative increase of the proton yield in the range of 3-4 MeV (Fig.3b).This may be due to the $p(g_{9/2}) \rightarrow n(g_{7/2})$ transition with the production of a three-quasiparticle state $[n g_{7/2}, p g_{9/2}^{-1}]_{1^+} n d_{5/2}$

Measurements with good resolution allow to explore the problem of the simple state distribution over the levels of complicated structure. As an example, let us consider the analysis of the fine structure of the Te^{III} proton spectrum. Measurements with a 30 KeV resolution have revealed I8 pronounced peaks in the range of 2-3.5 MeV [3,4].Fig.4 shows the distribution of the relative intensities of the fine structure groups after normalization to the averaged spectrum[5]. The experimental curve fits well with the χ^2-distribution for the number of degrees of freedom n=9±3. It is reasonable to assume the number of degrees of freedom to be equal to about the average number of levels related to the peak in the spectrum. According to our semi-empirical estimate the level density of Sb^{III} for appropriate spin values ($3/2^+$ and $5/2^+$) is 6.10^2 MeV^{-I} at the excitation energy E^* = 4.3 MeV (E_p= 2.5 MeV) and $2.6.10^3$ MeV^{-I} for

E^{*} = 5.3 MeV (E_p = 3.5 MeV). Thus, if all these levels were involved in the beta decay the number n would be expected to be 60 - 80. But this is not, indeed, the case. Only about I5 % of the levels with spin values corresponding to the allowed transition takes part in the beta decay. It means that the beta decay strength does not spead over all the states with given spin and parity. This fact is likely to indicate that up to excitation energies of, at least, 5.3 MeV the states are not completely mixed up.

We note that the analysis of the proton spectra of the tellurium isotopes is facilitated by that the proton decay goes mainly to the ground state of the final nucleus.

We also indicate another aspect of the study of the fine structure of the proton spectrum. A comparison of the spectra in coincidences with positons and without coincidences may give us useful information on the $\beta^{+}/_{K}$ branching ratio. The ratio of the both spectra is directly defined by $\beta^{+}/_{K}$ as a function of the transition energy.[8)]

II. SEARCH FOR THE PROTON DECAY FROM THE GROUND STATE

2.I. Introduction

The proton decay from the ground state was predicted long ago and there are no reasons to doubt that it exists, in principle. The discovery of this effect is of fundamental importance since the proton decay is the simplest mode of decay. The energy and half-life measurements will make it possible to determine the reduced proton width which is

calculated by nuclear models. Up to now the spectroscopic factors which are related to the reduced width were measured in nuclear reactions , the former being very sensitive to the reaction model employed. The proton decay studies may yield nuclear information of the same kind, as the alpha decay but the proton decay mechanism is not complicated with the process of the emitted particle formation. The proton decay will give very important evidence on the nuclear mass surface since the proton-active isotopes are extremely removed from the stability line in favor of the neutron deficiency.

Where should one look for the proton-unstable isotopes ?

The available predictions made by means of various mass formulas differ strongly from one another. Thus, for example, the boundary of the region of the proton-active nuclei ($B_p = 0$) predicted by different mass tables varies by 6-7 mass units for $Z > 50$, Fig.5. It is only a check in the region of considerable neutron deficiencies that will make it possible to choose formulas for a more correct prediction of the nuclear decay energies near the proton stability line. Data on delayed protons in the region of tellurium are in the best agreement with the tables by Garvey et al[14], Nemirovski[15] and Zeldes et al.[13]. In the middle of the rare-earth elements the Zeldes' table essentially differ from the calculations of other authors by that the former contains probably overestimated binding energies. Our estimates are based on the mass tables of

Garvey et al. and Nemirovski.

Fig. 6 gives the calculated energies of the proton decay of the isotopes of odd elements in the range of $Z > 50$. For even Z, due to the pairing effect, the proton instability boundary is biased in favor of large neutron deficiency. Also shown are the proton decay energies corresponding to half-lives of I sec, 3.10^{-4} sec and 10^{-6} sec (the orbital angular momentum escaped by the proton was chosen to be $2\hbar$). For the half-lives longer than I sec, of importance may be the β^+ decay competition. The half-life of 10^{-6} is the shortest one which is detectable by the technique used. Thus, the proton decay can, in principle, be observable if its energy falls within the gap $E_{min} \leq Q_p \leq E_{max}$. The size of this gap is not large (about 400 KeV for Z=65) and increases with increasing Z. This was one of the reasons to choose for the search the region of $Z > 50$. Another reason is associated with the reaction cross sections. It should be expected that the cross sections for the heavy-ion induced reactions resulting in proton-active isotopes are a small fraction of the total ones, due to the competition between the neutron and proton evaporation. This competition is less important for isotopes with large Z, that is the cross sections with emission of a given number of neutrons should increase with Z. Next, it should be expected that the cross section for the reaction (HI; p.xn) is larger than that for the case of evaporation of x neutrons alone. On the one hand, this is due to the fact that $\Gamma_p/\Gamma_n > 1$ for

nuclei with large neutron deficiency, on the other hand, the neutron evaporation cascade ends at an energy when a proton can escape.

According to our estimate[16], the (HI; p.6n) reaction cross section for production of proton-unstable isotopes in the range of tellurium must be about 2.10^{-30} cm^2. According to the Macfarlane systematics[4], the cross section of the (HI; p.6n) reaction for the production of ultra-neutron-deficient isotopes in the rare-earth region is expected to be not smaller than 10-20 μb. Thus, experimentally the problem reduces to the search of short-lived (< 1 sec) emitters of soft protons (Q_p = 0.5 - 1.5) MeV under the condition of a very intensive β-background.

2.2. Experimental

In our experiments a gas-filled mass separator was used to ensure a rapid (10^{-6} sec) separation of the reaction products from the beam. It was first been suggested by Fulmer and Cohen[17] and then used in fission fragment studies[18]. A diagram of the apparatus is shown in Fig.7. A target is located at the point of the magnetic system source and irradiated with a multicharged ion beam of the JINR U-300 cyclotron. Recoils are ejected from the target as ions in a narrow cone in the beam direction.

Passing through the magnetic system filled with a gas (for example, helium at p = 2 torr) recoils undergo collisions with the gas molecules and change their charge in a statistical manner. Accordingly, the radius of curvature

changes, as well. However, the radius of curvature averaged over all the path will be close to the value corresponding to a recoil with equilibrium charge $\bar{e}$. The deflection of the "equilibrium" particle in the magnetic field is practically independent of the velocity. Owing to multiple charge exchange collisions, the fluctuations of the average radius of curvature with respect to the mean value are found to be significantly smaller than $\frac{\Delta e}{\bar{e}}$. For example, for A=100, the resolution $\frac{\Delta H\rho}{\langle H\rho \rangle}$ is about 3% in the case of helium filling *).

After passing through the mass separator recoils penetrated into a stopping volume throughout a vacuum-tight organic film about 200 $\mu g/cm^2$ thick. This volume is located inside a telescope consisting of three coaxial proportional counters. The first and second counters are separated from the stopping volume and from each other with an organic film 50 $\mu g/cm^2$ thick powdered with gold. The third counter is separated from the second one by an aluminium foil 8 μ thick. The stopping volume radius is 35 mm, the radial thicknesses of the counters are 12 mm, 140 mm and 20 mm, respectively. The telescope is filled with a mixture of argon and methan (5%) at a presure of 100-150 torr. The first counter (ΔE -counter) measures the specific ionization of particles emitted by decaying recoils , the second one

---

*) A detailed description of a gas-filled mass separator on a heavy-ion beam is given in refs.[19,20].

(E-counter) measures the residual energy for particles stopped in it. The amplitude analysis is gated by a pulse corresponding to the coincidences between the first and second counters and to anticoincidences with the third one. Thus, the particle stopped in the second counter are extracted and the background due to delayed protons is essentially eliminated. The electronic devices used make it possible to measure simultaneously the amplitudes of the pulses from the Δ E-and E-counters and the time of their emergence after the beam burst. The analyzer input was blocked for the beam burst time. The detectable half-lives range from 3.10^{-4} to I sec.

The total efficiency was measured by means of the well known alpha emitter, Dy^{150}, which was produced by the reaction $Sn^{124}(S^{32},6n)$. It was found to be about 10^{-3}. For the available beam intensities one should expect 10 events per hour for a cross section of about 10^{-30} cm^2. To calibrate the mass separator use was made of the known radioactive isotopes produced by heavy ions. Besides, in some cases recoils were detected either directly by mica detectors or by a compensation chamber[19].

2.3. Results of Experiments

In our experiments targets from enriched isotopes Ru^{96}, Pd^{102}, Cd^{106} and Sn^{112} were bombarded with $^{+6}S^{32}$ ions. The isotopes Ru^{96} and Sn^{112} were also irradiated with $^{+6}Cl^{35}$ ions.

To test the reliability of the techniques used measure-

ments of delayed protons have been performed. In these experiments the detection of the Δ E-and E-spectra was gated by triple coincidences which suppressed almost completely the beta background. Fig.8 shows the yield of delayed protons which were produced in the reactions $Ru^{96} + S^{32}$, $Ru^{96} + Cl^{35}$, $Sn^{II2} + S^{32}$ and $Sn^{II2} + Cl^{35}$ as a function of the magnetic rigidity. We have not spent much effort to identify definitely these delayed proton emitters. However, we can say that the peaks of the yield curves are located at the $H\rho$ values which are close to the calculated ones[19] for the rare-earth isotopes produced in the above reactions. These are Ce-Nd isotopes with mass number around 123 for the $Ru^{96} + S^{32}$ reaction and Gd-Dy isotopes with mass number around 139 for the $Sn^{II2} + S^{32}$ reaction. With increasing Z the yield is reduced due to decreasing of β^+/β^+ branching ratio.

Fig. 9 gives the two-dimensional spectrum for delayed protons produced in the reaction $Ru^{96} + S^{32}$. The calculated line shows the energy loses in the Δ E-and E-counters for protons emitted radially from the axis of the stopping volume. Protons of an energy higher than I.0 MeV (at p= I00 torr) did not stop in the second counter, therefore at this point the slop of the curve sharply changes. The delayed proton pulses are grouped in the region of small amplitudes since the energy of the main fraction of them exceeds 2 MeV. The half-life of this activity was found to be about 2 sec. It is quite possible that this is a mixture of a few emitters.

In the experiments on the search for soft-proton emitters we have used a coincidence-anticoincidence circuit for obtaining the gate-pulse. In this regime there is a considerable beta background in the region of small amplitudes (the formation cross section for beta-active isotopes is about equal to the total one). The advanatge of this regime consists in that the danger of electromagnetic noise is essentially reduced and the counting rate for the majority of delayed protons depressed by about a factor of 20.

Fig. 10 presents the Δ E-E spectrum from the bombardment of a Pd^{102} target with 210 MeV S^{32} ions. A large number of pulses in the region of small amplitudes is shown to be due mainly to the beta activity. There is no pulse in the region of the amplitudes corresponding to the protons with $E_p < 1.5$ MeV.

Fig. 11 gives the ΔE - E spectrum measured when bombarding Ru^{96} with 190 MeV S^{32} ions. An intensive beta background is again seen in the left lower corner of the plane. In addition, there are a few pulses which may be assigned to protons of an energy lower than 1.2 MeV. A detailed analysis of all the possible background sources has shown that the most serious danger may be caused by the delayed protons the yield of which is 100 times larger than that for soft protons. The maximum of the delayed proton spectra is expected to be at an energy of 3.0 - 3.5 MeV. However, for proton binding energy close to zero this spectrum may have a tail in the energy region $E_p \leqslant 1.2$ MeV. However the

extrapolation of the spectra of delayed protons to the low energy region shows that the effect observed cannot be completely attributed to them. At least, half of this effect is not due to the delayed proton background. The half-life of this excess activity is found to be $0.2 \text{ sec} \leqslant T_{I/2} \leqslant 2 \text{ sec}$. This conclusion is supported by the fact that there is a difference in the beam energy dependence of the soft and delayed proton yields. The increase of the beam energy from I90 to 2I0 MeV results in the decrease of the soft proton counting rate by a factor of 2 - 3, while the delayed proton yield grows by a factor of I.5 (see Table II).

The results obtained in irradiating various targets with S^{32} and Cl^{35} ions are summarized in Table II. The fifth column contains the counting rate for pulses which may be attributed to soft protons ($E_p \leqslant$ I.2 MeV). The last column contains the cross section corresponding to this counting rate. The maximum yield of soft protons was observed for the reaction $Ru^{96} + S^{32}$. The counting rate for other target-projectile combinations is too small for any test measurements to be performed.

We interprete the data obtained as an indication that in the reaction $Ru^{96} + S^{32}$ a nucleus is produced which decays by emission of a 0.7 - I.0 MeV proton. This isotope may be Pr $^{I23-I22}$. We are planning additional experiments which would lead us to more definite conclusions.

The authors are indepted to Prof. G.N.Flerov for his continuous interest in this work and the support.

REFERENCES

I). V.A.Karnaukhov, G.M.Ter-Akopian, V.G.Subbotin (I962), Dubna Report P-I072; Proceedings of the Third Confe - rence on Reactions between Complex Nuclei,Asilomar, USA, I963, p.434.
R.Barton,R.McPherson et al.,Bull.Am.Phys.Soc.8,357(1963)
R.Barton,R.Bell et al.,Can.J.Phys.41,2007(1963)

2). P.Hornshoj, K.Wilsky. P.G.Hansen, B.Jonson, M.Alpsten, G.Anderson, Aa.Appelquist, B.Bengtsson, O.B.Nielsen (to be published).

3). D.D.Bogdanov, Sh.Darotzi, V.A.Karnaukhov, L.A.Petrov, G.M.Ter-Akopian, Yader. Fiz., 6,893 (I967).

4). R.Macfarlane, Ark. für Fysik, Bd 36,43I(I967).

5). V.A.Karnaukhov, Yader, Fiz., I0 (I969), 450.

6). J.I.Fujita, K.Ikeda, Nucl.Phys., 67, I45 (I965).
J.I.Fujita, Y.Futami, K.Ikeda, Proc. Inter.Conf.on Nuclear Structure, Tokyo (I967).

7). M.Yamada, Bull.Sci.Eng. Res.Lab., Wased Univ. No 3I/32 I46 (I965).
K.Takahashi, M.Yamada, Prog.Theor.Phys., 4I, I470(I969)

8). I.Bacho, D.D.Bogdanov, Sh.Darotzi, V.A.Karnaukhov, L.A. Petrov, Yader. Fiz., 7, II53 (I968).

9). A.G.W.Cameron, At Energ.Canad. Ltd.Report CRL4I,I957.

I0).P.Seeger, Preprint LA-3380, I965.

II).W.Swiatecki, W. Myers, UCRL-II980,I965.

I2).J.Wing, J.D.Varley, ANL-6886, I964.

I3).N.Zeldes, A.Grill, A.Simievic, Mat.Fys.Skr.Dan.Vid.Sels 3, No 5 (I967).

I4).G.T.Garvey, I.Kelson, I.Talmi, R.L.Jaffe, W.J.Gervace, Rev.Mod.Phys., 4I, No 4 P II (I969).

I5). P.E.Nemirovski, private communication (1968)

I6). L.S.Vertogradov, V.A.Karnaukhov, L.A.Petrov, G.M. Ter-Akopian, Nucl.Phys., A90, 23 (I967).

I7). C.B.Fulmer, B.L.Cohen, Phys.Rev., I09, 94(I958).

I8). P.Armbruster, Nucleonik, 3, I88 (I96I).

I9). I.Bacho, D.D.Bogdanov, Sh.Darotzi,V.A.Karnaukhov, L.A.Petrov, G.M.Ter-Akopian, Prib.Tekh.Exper., 2, 43(I970).

2o). L.A.Petrov, V.A.Karnaukhov, D.D.Bogdanov, JETP (to be published).

REACTION	ISOTOPE	E MeV BEAM	HI-FULL FLOW IO^{15}	$\frac{N_p}{IO^{15}HI}$	$\frac{N_{dp}}{IO^{15}HI}$	σ mb
$Ru^{96}+Cl^{35}$	Pm^{125}	215	2,5	3	230	0,3
	Pm^{126}					
$Pd^{102}+S^{32}$	Pm^{127}	210	6	0	-	<0,02
$Ru^{96}+S^{32}$	Pr^{122}	210	6	I	500	0,I
	Pr^{123}	I90	22	3	320	0,3
$Cd^{106}+S^{32}$	Eu^{131}	240	I9	0,5	-	0,05
	Eu^{132}	210	2	2	-	0,2
	Eu^{133}	I90	I	0	-	<0,I
$Sn^{112}+S^{32}$	Tb^{136}	250	I	0	I0	<0,I
	Tb^{137}	225	8	0,5	25	0,05
	Tb^{138}	200	7	I	50	0,I
$Sn^{112}+Cl^{35}$	Ho^{141}	230	2,5	2	II0	0,2
	Ho^{142}	210	I	I	75	0,I
	Ho^{143}	I70	0,6	0	20	<0,2

Table II

N_p - the number of pulses which may be caused by protons with $E_p < I.2$ MeV.

N_{dp} - the number of detected delayed protons

The last column is the cross section corresponding to the counting rate of N_p.

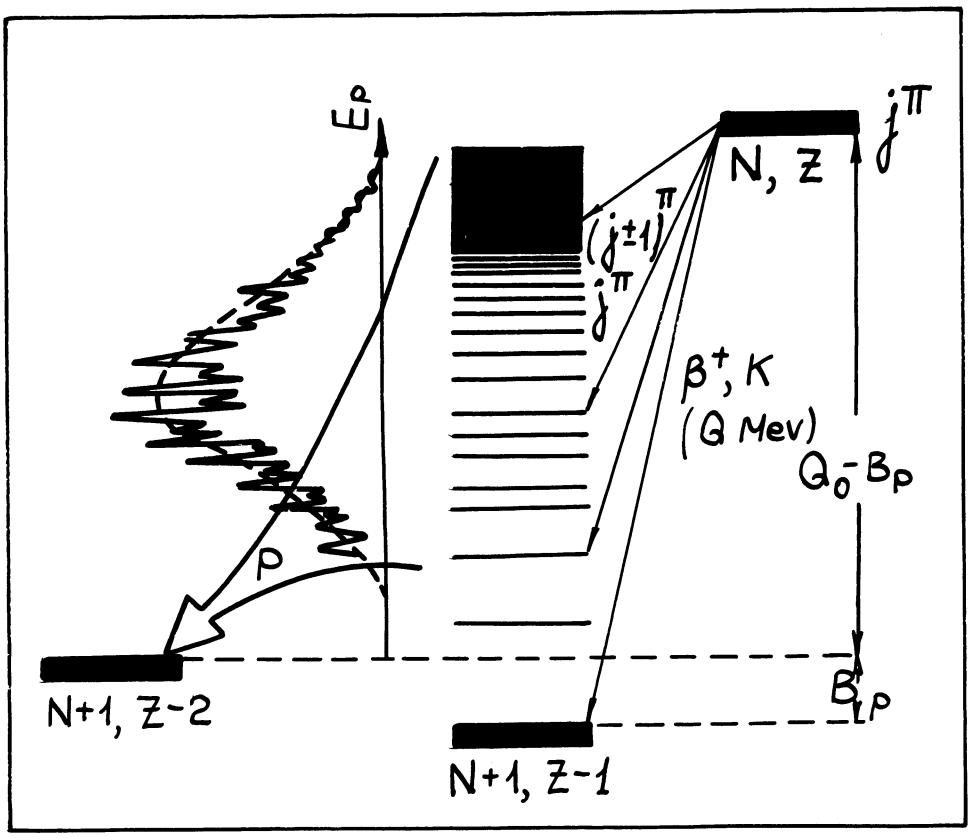

Fig.I

Illustative scheme of the decay reasulting in delayed proton emission.The averaged proton spectrum has the shape of a broad peak. For a sufficiently high resolution the spectrum exhibits the fine structure related to the daughter nucleus levels.

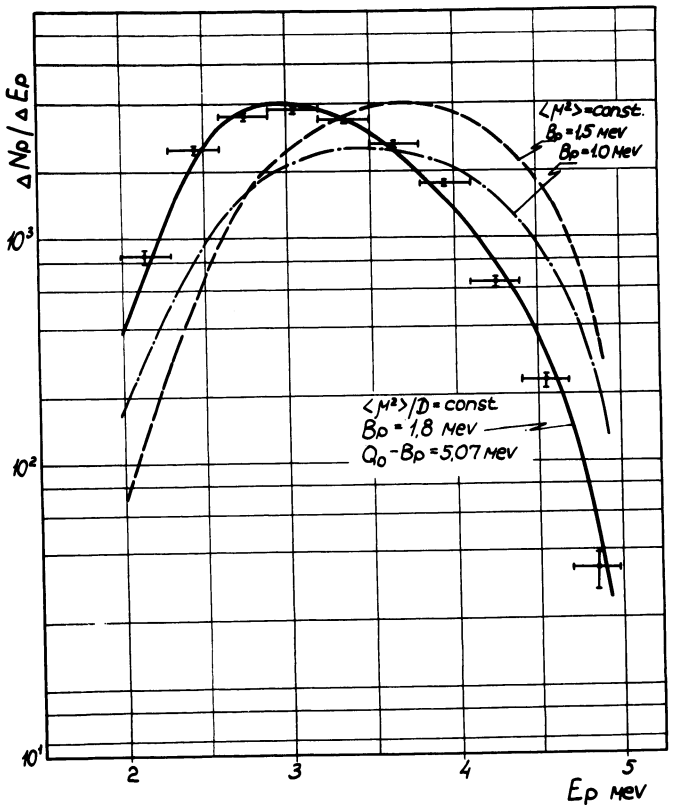

Fig. 2a

Averaged spectrum of delayed protons of Te^{III}. The continuous curve is calculated under the assumption that the beta decay strengh function is constant. In the calculation the value $Q_0 - B_p = 5.07$ MeV is used, determined by measuring $\beta^+ - p$ coincidences. The best agreement with experiment is obtained at $B_p = 1.83$. The dashed line is the calculation under the assumption $\langle M^2 \rangle = \text{const.}$

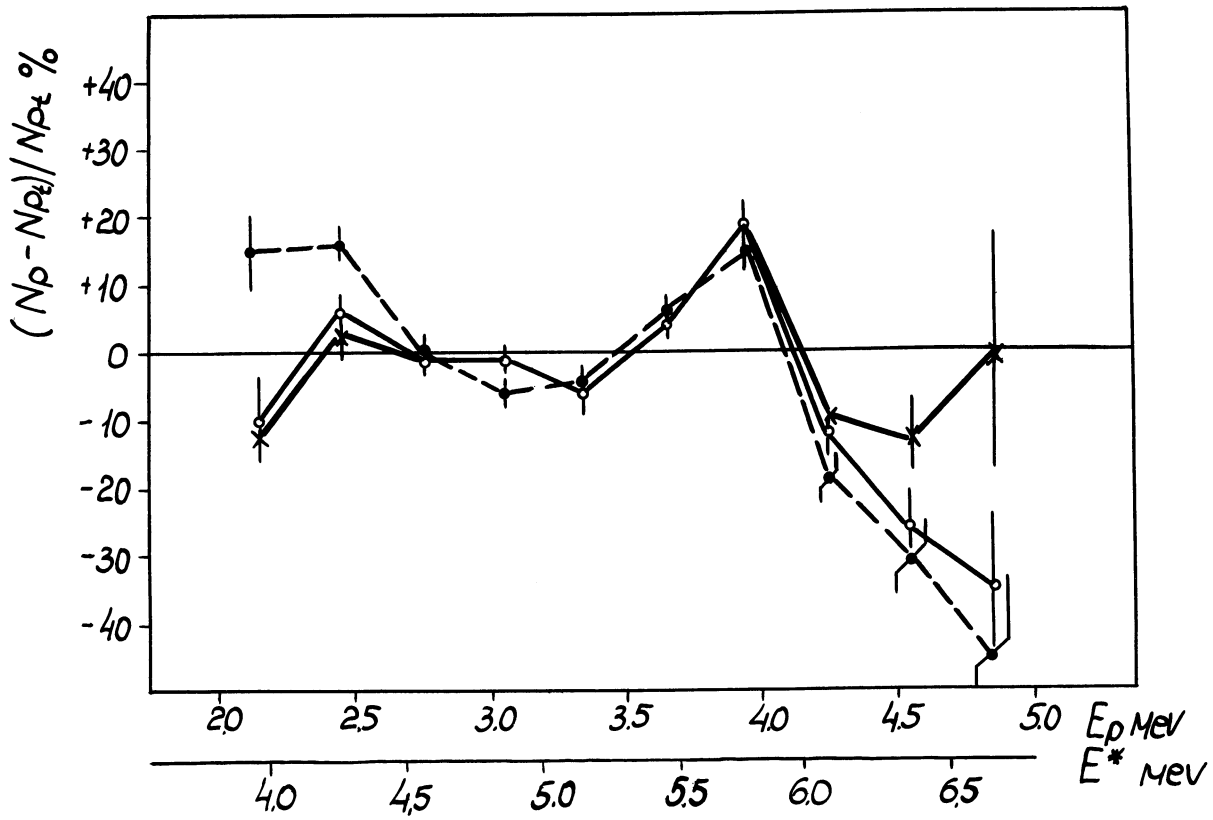

Fig. 2b

Comparison of the calculated shape of the averaged spectrum of the delayed protons of Te^{III} with experiment.

- ● the calculation under the assumption $\langle M^2 \rangle / D$ = const.
- o the calculation under the assumption of the resonance behaviour of $\langle M^2 \rangle / D$

  $Q_o - B_p = 5.07$ MeV
- × The same, but $Q_o - B_p$ is 5.0 MeV.

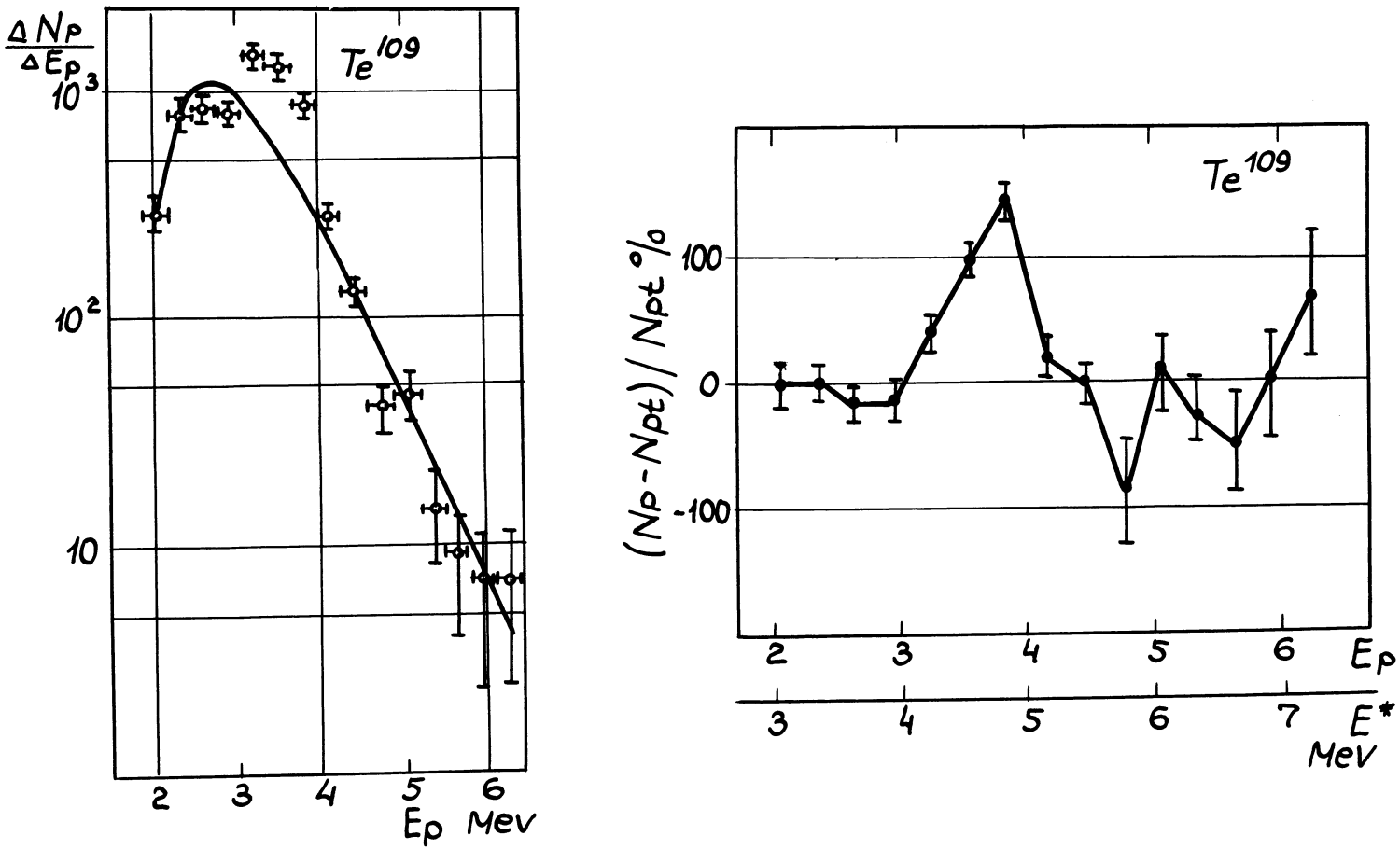

Figs. 3a and 3b

a. Averaged spectrum of the delayed protons of Te^{I09}.
The calculation for B_p = I.0 MeV, $Q_o - B_p$ = 7.6 MeV

b. Comparison of the calculated shape of the delayed protons of Te^{I09} with experiment.

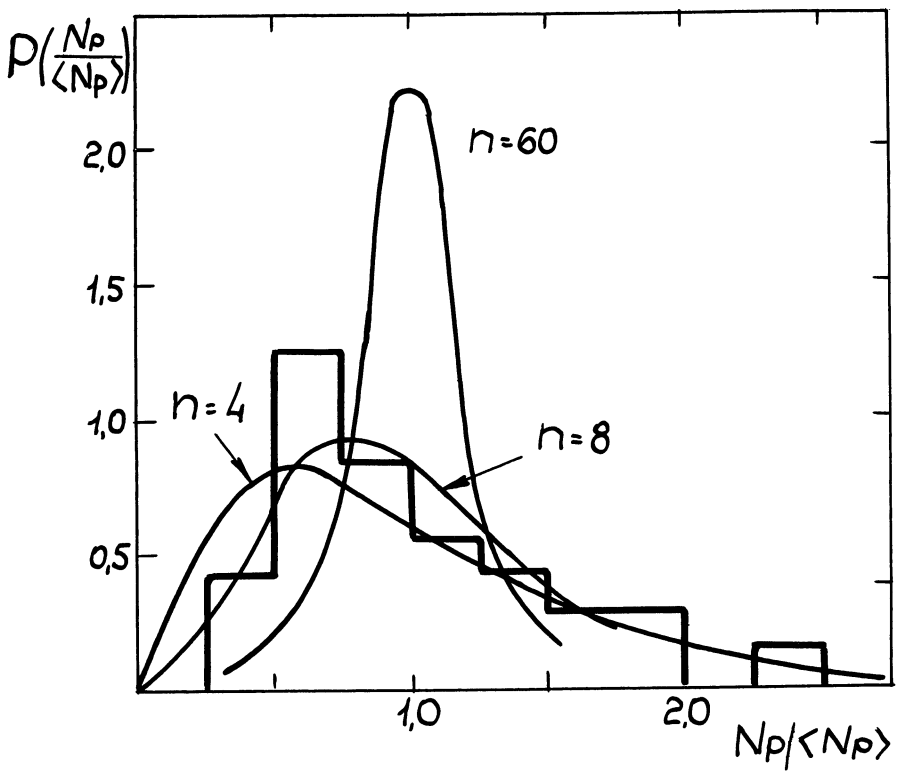

Fig. 4

Distribution of the relative intensities of groups in the proton spectrum with a 30 KeV resolution after normalization. The continuous curves are the χ^2 distribution with the indicated number of degrees of freedom.

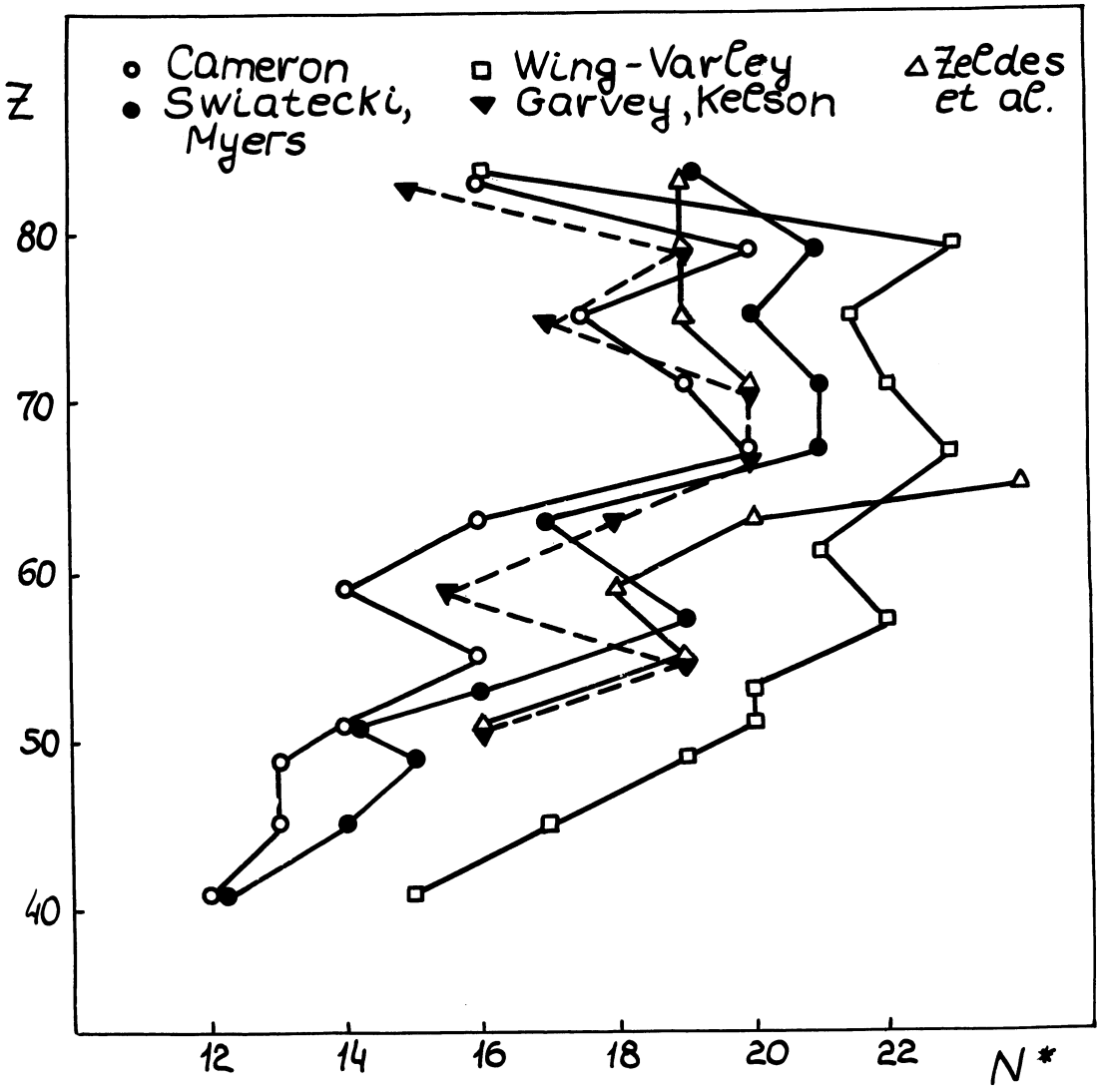

Fig. 5

Proton unstability lines calculated by some mass formulas for odd elements.

The number of neutrons which should be removed from a light stable isotope for reaching the isotope with $B_p=0$ is reconed on the ordinate axis.

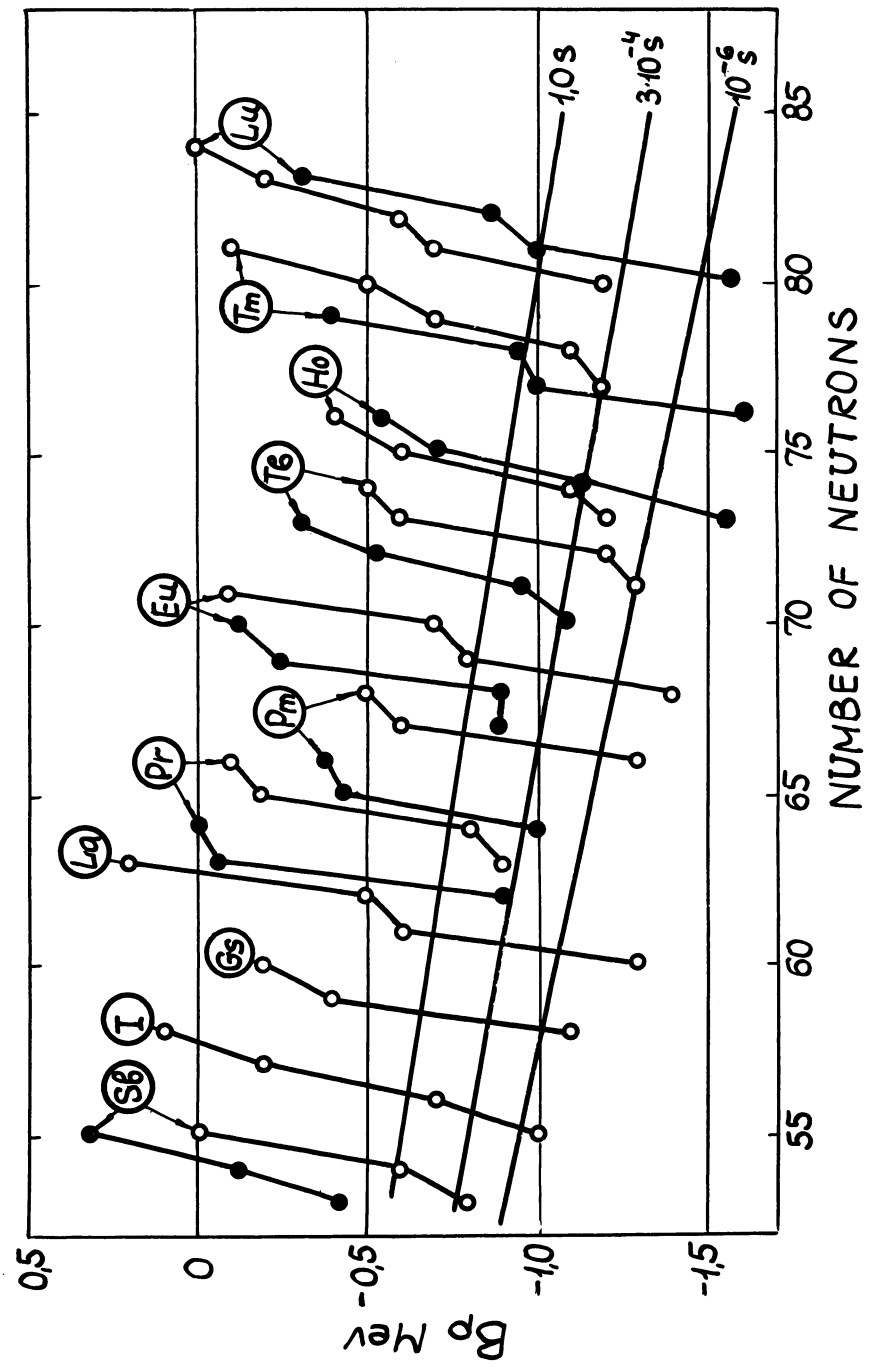

Fig. 6

Proton decay energies according to the Nemirovski (o) and Garvey-Kelson's (•) calculations. The lines labelled as I sec, 3.10^{-4} sec and 10^{-6} sec are plotted through the energies corresponding to these half-lives for $\ell_p = 2\hbar$ proton emission.

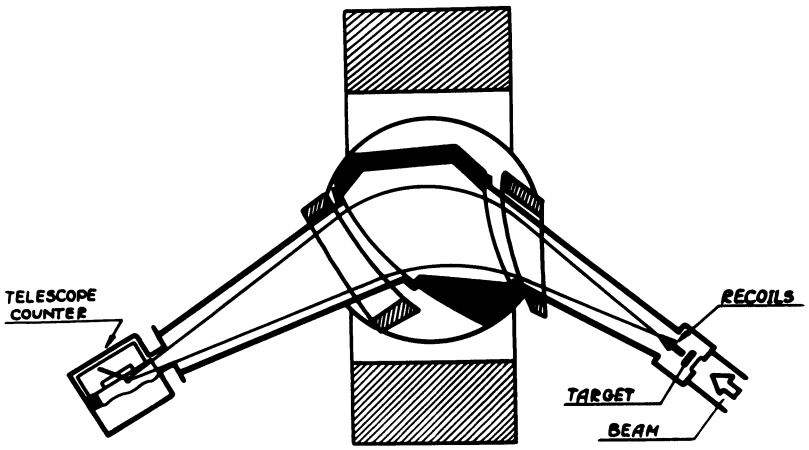

Fig. 7

Diagram of the gas-filled separator with a telescope consisting of proportional counters.

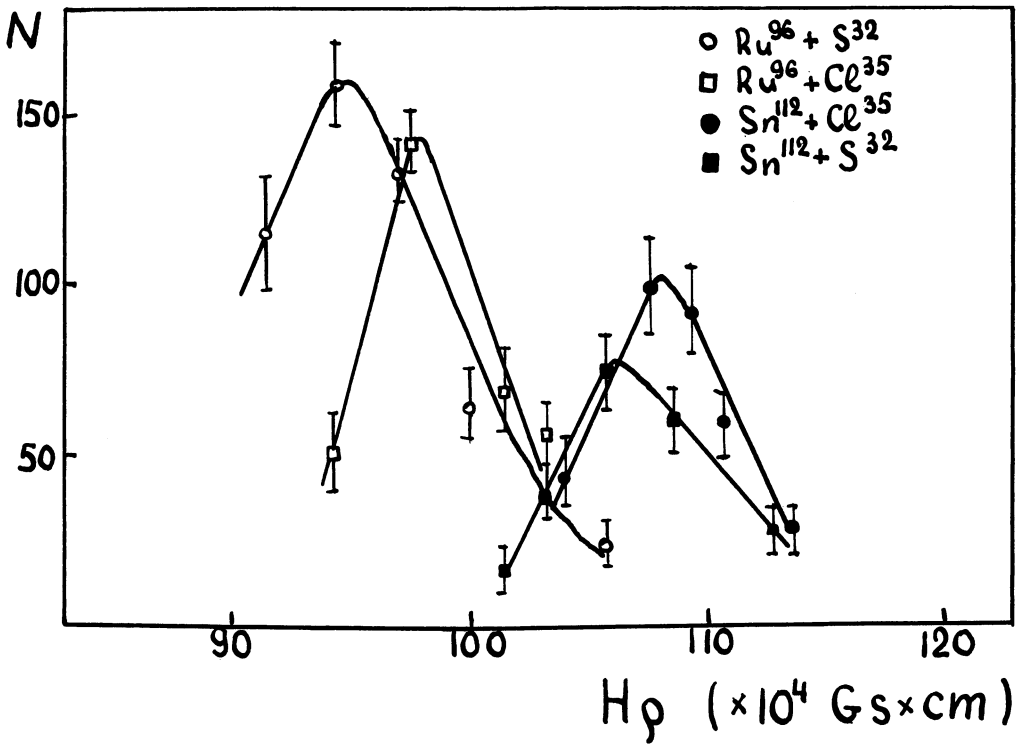

Fig. 8

Delayed proton counting rate as a function of the magnetic rigidity. For Ru^{96} target the separator is filled with helium (p= I.5 torr). For Sn^{II2} target - with a mixture of helium (75%) and air (25%) at p= I.I torr. The energy of S^{32} and Cl^{35} ions is about 2I0 MeV. Full flow of ions for Ru-target is $3.I0^{I4}$; for Sn target is $I0^{I5}$.

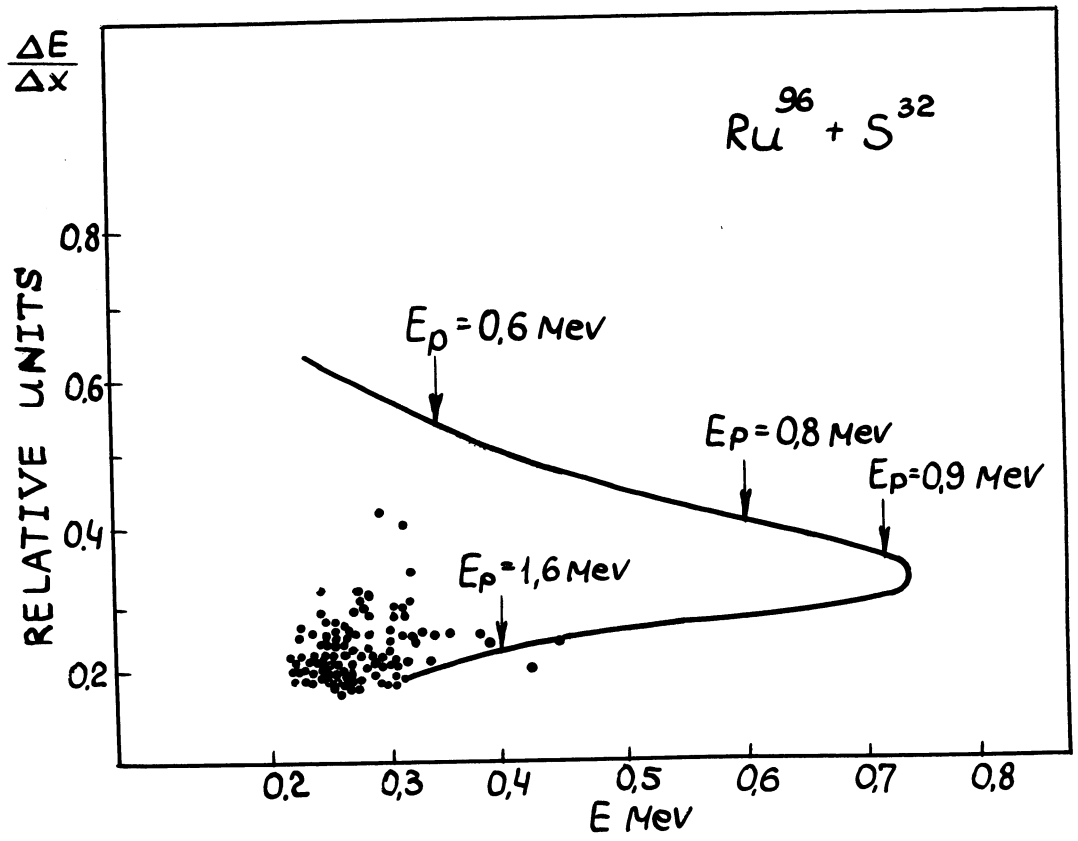

Fig. 9

ΔE - E delayed proton spectrum for the case Ru^{96}+ S^{32} (E= I90 MeV). The pulse detection was gated by triple coincidences. The calibration curve is calculated for protons emitted radially from the stopping volume axis.

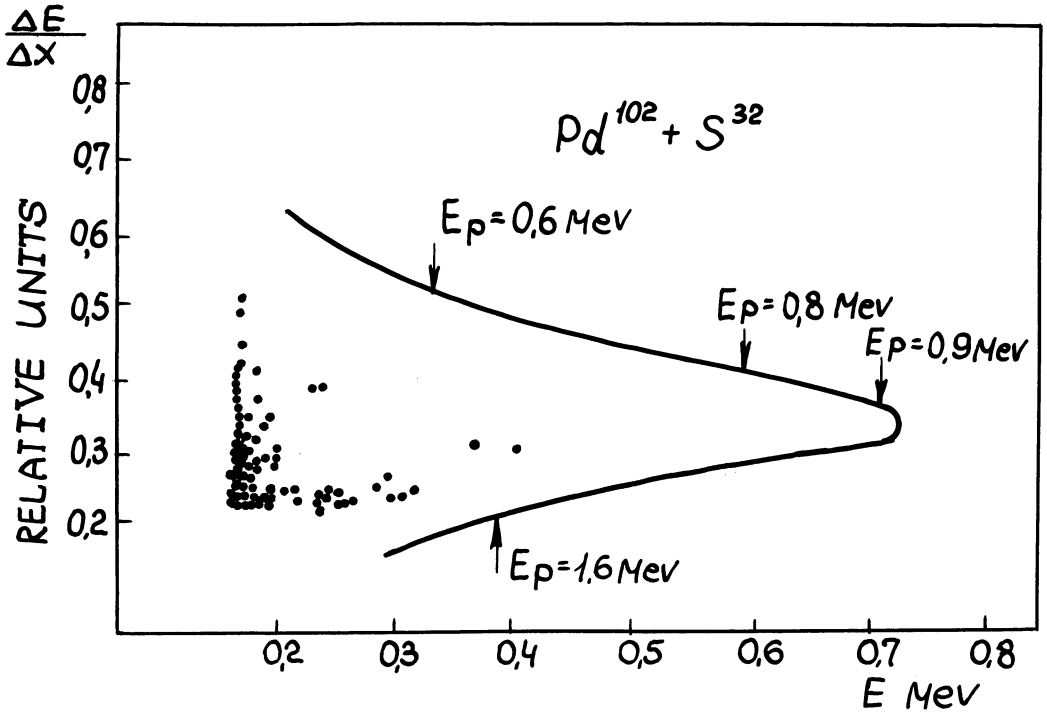

Fig. I0.

Δ E - E spectrum for particles stopped in the E-counter;

bombardment of Pd^{I02} with S^{32} ions

$E(S^{32})$ = 2I0 MeV - 6 hour irradiation.

The pulse detection was gated by coincidences of Δ E and E- counters under the condition of anticoincidence with the third counter.

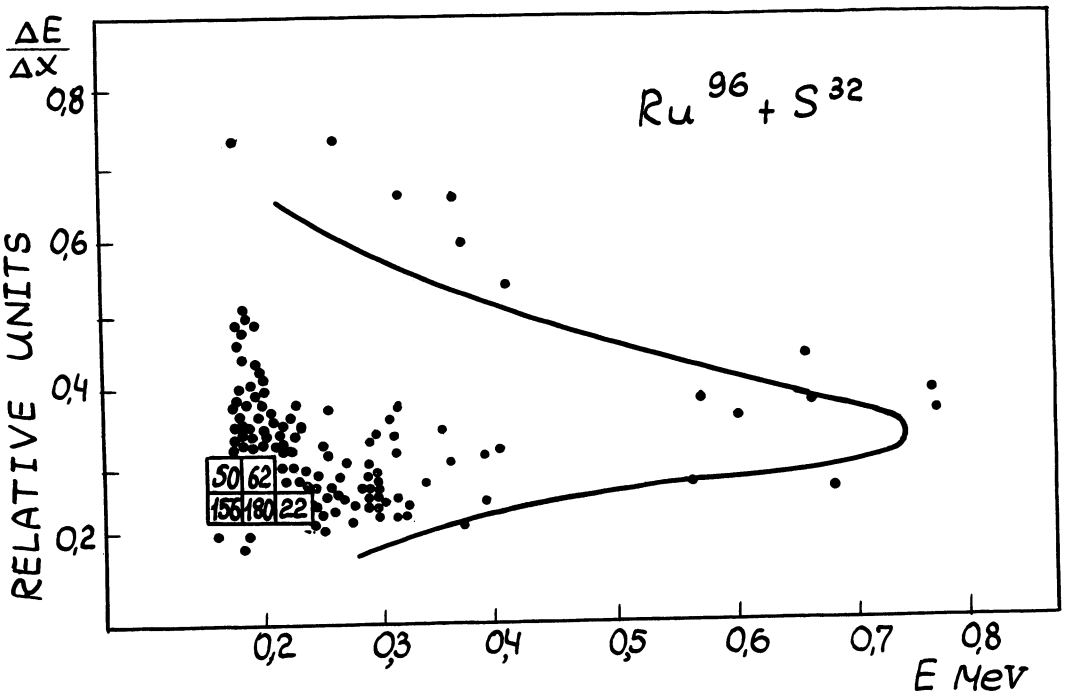

Fig. II.

ΔE - E spectrum for particles stopped in the E-counter. bombardment of Ru^{96} with S^{32} ions;

$E(S^{32})$ = I90 MeV - 7 hour irradiation

The pulse detection was gated by coincidences of ΔE and E-counters under the condition of anticoincidence with the third counter.